PRODUCTION OF A HIGGS-BOSON PAIR IN e^-e^+-COLLISIONS (II)

S.K. ABDULLAYEV, M.Sh. GOJAYEV
Baku State University, Azerbaijan,
AZ 1148, Baku, st. Z. Khalilova, 23, m_qocayev@mail.ru

Within the framework of the Standard Model and taking into account arbitrary polarizations of the electron-positron pair, the differential cross section of the process $e^-e^+ \to ZHH$ is calculated taking into account all Feynman diagrams. The characteristic features in the behavior of the cross section and polarization characteristics (left-right spin asymmetry, transverse spin asymmetry) depending on the angles of departure and the energies of the particles are investigated and revealed.

Keywords: Standard model, electron-positron pair, Higgs boson pair, left-right spin asymmetry, transverse spin asymmetry.
PACS: 13.66.Fg, 14.70.Hp, 14.80.Bn.

1. INTRODUCTION

The Standard Model (SM), based on local gauge symmetry $SU_C(3)\times SU_L(2)\times U_Y(1)$, satisfactorily describes the physics of strong and electroweak interactions of quarks, leptons and gauge bosons [1-3]. A doublet of scalar fields $\varphi=\begin{pmatrix}\varphi^+\\ \varphi^0\end{pmatrix}$ is introduced into the theory, the neutral component of which has a vacuum value other than zero. As a result of spontaneous symmetry breaking due to quantum excitations of the scalar field, a Higgs boson H appears, and due to interaction with this field, charged leptons, quarks and gauge bosons $W^{\pm}$ and Z^0 acquire mass. This mechanism of particle mass generation is known as the mechanism of spontaneous violation of the Brauth-Englert-Higgs symmetry.

The discovery of the Higgs boson with characteristics corresponding to SM predictions was carried out by ATLAS and CMS collations in 2012 at the Large Hadron Collider (LHC) at CERN [4, 5] (see also reviews [6-8]). With the discovery of the Higgs boson H with a mass of about 125 GeV, the missing particle in SM was found, and this began a new period in the study of the properties of fundamental interactions. In this regard, theoretical and experimental interest in various channels of the Higgs boson production and decay has greatly increased.

Due to the rather strong connection of the Higgs boson with vector Z- and W-bosons, the main sources of the production of Higgs bosons are the radiation of their Z- and W-bosons born in various experiments. A particularly intense source of Higgs bosons could be the processes occurring in electron-positron collisions. Note that collisions of high-energy electrons and positrons are an effective method for studying the mechanisms of interaction of elementary particles. This is due to the following circumstances. Firstly, the interaction of an electron-positron pair is described in SM, so the results obtained are well interpreted. Secondly, since the electron-positron pair does not participate in strong interactions, the background conditions of experiments are significantly improved compared to the studies conducted in the LHC with proton-proton beams. Note that high-energy electron-positron colliders have either been designed or are scheduled to be designed in various laboratories around the world [9, 10].

The process of the Higgs boson generation in electron-positron collisions $e^-e^+ \to ZH$ is considered in a number of papers [2, 11-14]. Here we consider the process of the generation of the Higgs boson of a pair in arbitrarily polarized electron-positron collisions

$$e^- + e^+ \to Z^* \to Z + H + H\,, \qquad (1)$$

where Z^* is the virtual Z-boson. In the case of an unpolarized electron-positron pair, this process is considered in [2, 15, 16].

An analytical expression for the differential effective cross section of the reaction (1) is obtained within the SM and taking into account arbitrary polarizations of the electron-positron pair. Left-right and transverse spin asymmetries due to the polarizations of the electron-positron pair are determined. The dependence of the asymmetries and the effective cross-section of the process on the departure angles and particle energies is studied in detail.

2. CALCULATION OF DIAGRAMS c) AND d)

The process $e^-e^+ \to ZHH$ is described by Feynman diagrams shown in Fig. 1 (4-particle momentums are written in parentheses). The calculation of diagrams a) and b) was carried out in the first part of this work [17]. Calculations of diagrams c) and d), as well as interference of all diagrams, are also carried out here.

The amplitude corresponding to diagram b) can be written as:

$$M_c = g_{Zee}g^2_{ZZH}\ell_\mu D_{\mu\nu}(p)D_{\nu\rho}(q)U^*_\rho(k)\,, \qquad (2)$$

131, H.Javid ave, AZ-1143, Baku
Institute of Physics
E-mail: jophphysics@gmail.com

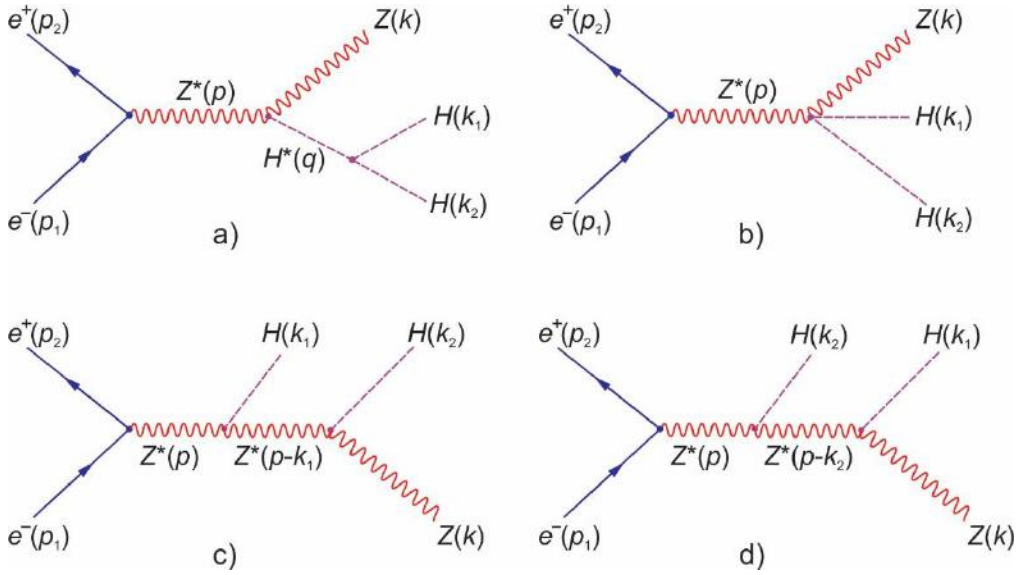

Fig. 1. Feynman diagrams of process $e^-e^+ \to ZHH$

where

$$\ell_\mu = \bar{\upsilon}(p_2, s_2)\gamma_\mu[g_L(1+\gamma_5) + g_R(1-\gamma_5)]u(p_1, s_1) \tag{3}$$

– electron-positron weak neutral current; s_1 and s_2 4-polarization vectors of electron and positron; g_L and g_R – left and right electron Z-boson coupling constants.

$$g_L = -\frac{1}{2} + x_W, \quad g_R = x_W; \tag{4}$$

$x_W = \sin^2\theta_W$ – Weinberg parameter (θ_W – Weinberg angle);

$$g_{Zee} = (\sqrt{2}G_F)^{1/2} M_Z, \; g_{ZZH} = 2(\sqrt{2}G_F)^{1/2} M_Z^2 \tag{5}$$

– constants of electron-Z-boson and Higgs boson-Z-boson interactions; $D_{\mu\nu}(p)$ and $D_{\nu\rho}(q)$ are vector Z-boson propagators

$$D_{\mu\nu}(p) = i\left(-g_{\mu\nu} + \frac{p_\mu p_\nu}{M_Z^2}\right)\cdot\frac{1}{p^2 - M_Z^2},$$

M_Z – the mass of the Z-boson; G_F – the Fermi constant of weak interactions; $p = p_1 + p_2$ and $q = p - k_1 = k + k_2$ – the total 4-momenta of the electron-positron pair and the Z-Higgs boson system; $U_\rho^*(k)$ – the 4-polarization vector of the vector Z-boson.

At high energies of the electron-positron pair ($\sqrt{s} >> m$, $\sqrt{s}$ – the total energy of the e^-e^+-pair in the center-of–mass system, m – the mass of the electron), a weak electron current is preserved

$$p_\mu \ell_\mu = (p_1 + p_2)_\mu \ell_\mu = 0,$$

as a result, the amplitude (2) is greatly simplified:

$$M_c = g_{Zee} g_{ZZH}^2 \cdot \frac{1}{s(1-r_Z)} \cdot \frac{1}{s(y_1 + r_H - r_Z)} \cdot \ell_\nu \cdot \left(g_{\nu\rho} - \frac{q_\nu q_\rho}{M_Z^2}\right) U_\rho^*(k). \tag{6}$$

For the modulus of the square of the matrix element (6), the expression is obtained:

$$|M_c|^2=\frac{g_{Zee}^2}{s^2(1-r_Z)^2}\frac{g_{ZZH}^4}{s^2(y_1+r_H-r_Z)^2}L_{\mu\nu}\left(g_{\mu\sigma}-\frac{q_\mu q_\sigma}{M_Z^2}\right)\cdot\left(g_{\nu\rho}-\frac{q_\nu q_\rho}{M_Z^2}\right)\cdot\left(-g_{\rho\sigma}+\frac{k_\rho k_\sigma}{M_Z^2}\right). \quad (7)$$

Here $L_{\mu\nu}=\ell_\mu\bar{\ell}_\nu$ is the electron-positron tensor

$$L_{\mu\nu}=2(g_L^2+g_R^2)[p_{1\mu}p_{2\nu}+p_{2\mu}p_{1\nu}-(p_1\cdot p_2)g_{\mu\nu}-m^2(s_{1\mu}s_{2\nu}+s_{2\mu}s_{1\nu}-(s_1\cdot s_2)g_{\mu\nu})]+$$
$$+2(g_L^2-g_R^2)m[p_{1\mu}s_{2\nu}+p_{1\nu}s_{2\mu}-(p_1\cdot s_2)g_{\mu\nu}-s_{1\mu}p_{2\nu}-s_{1\nu}p_{2\mu}+(p_2\cdot s_1)g_{\mu\nu}]+$$
$$+4g_Lg_R[(p_1\cdot s_2)(s_{1\mu}p_{2\nu}+s_{1\nu}p_{2\mu}-(s_1\cdot p_2)g_{\mu\nu})+(p_2\cdot s_1)(p_{1\mu}s_{2\nu}+p_{1\nu}s_{2\mu})-$$
$$-(p_1\cdot p_2)(s_{1\mu}s_{2\nu}+s_{2\mu}s_{1\nu}-(s_1\cdot s_2)g_{\mu\nu})-(s_1\cdot s_2)(p_{1\mu}p_{2\nu}+p_{2\mu}p_{1\nu})]. \quad (8)$$

In formula (7), the tensor

$$\sum_{\text{pol.}}U_\rho^*(k)U_\sigma(k)=-g_{\rho\sigma}+\frac{k_\rho k_\sigma}{M_Z^2}$$

it arose due to the summation of the vector Z-boson by polarization states.

Due to the cumbersomeness of the expression, the product of the electron $L_{\mu\nu}$ and Z-boson tensors

$$L_{\mu\nu}\left(g_{\mu\sigma}-\frac{q_\mu q_\sigma}{M_Z^2}\right)\cdot\left(g_{\nu\rho}-\frac{q_\nu q_\rho}{M_Z^2}\right)\cdot\left(-g_{\rho\sigma}+\frac{k_\rho k_\sigma}{M_Z^2}\right)=$$
$$=L_{\mu\nu}\left[-g_{\mu\nu}+\frac{k_\mu k_\nu}{M_Z^2}+\frac{k_{1\mu}k_{1\nu}}{M_Z^2}\left(2-\frac{y_1+r_H}{r_Z}+\frac{(y_1+r_Z)^2}{4r_Z^2}\right)+\frac{k_\mu k_{1\nu}+k_\nu k_{1\mu}}{M_Z^2}\cdot\frac{y_1+r_Z}{2r_Z}\right],$$

it is not given here, we have introduced the notation:

$$r_Z=\left(\frac{M_Z}{\sqrt{s}}\right)^2,\ r_H=\left(\frac{M_H}{\sqrt{s}}\right)^2,\ y_1=1-x_1,\ x_1=\frac{2E_1}{\sqrt{s}},$$

E_1 – the energy of the Higgs boson with 4-momentum k_1.

The differential effective cross section of the reaction $e^-e^+\to ZHH$ corresponding to diagram b) of Fig. 1 is expressed by the formula (e^-e^+-the pair is arbitrarily polarized):

$$\frac{d^3\sigma_c}{dx_Z dx_1 d\Omega}=\frac{\sqrt{2}}{128\pi^4}\cdot\frac{G_F^3M_Z^6}{s(1-r_Z)^2}\cdot\frac{r_Z}{(y_1+r_H-r_Z)^2}\times$$
$$\times\{[(g_L^2(1-\lambda_1)(1+\lambda_2)+g_R^2(1+\lambda_1)(1-\lambda_2)]\cdot f_1+2g_Lg_R\eta_1\eta_2 f_2]\}, \quad (9)$$

where

$$f_1=x_Z^2(1-\upsilon^2\cos^2\theta)+4r_Z\upsilon^2(1+\cos^2\theta)+\left(2-\frac{y_1+r_H}{r_Z}+\frac{(y_1+r_Z)^2}{4r_Z^2}\right)[x_1^2(1-\upsilon^2\cos^2\theta_1)-$$
$$-4r_H\upsilon^2\sin^2\theta_1]+\frac{y_1+r_Z}{r_Z}[x_Zx_1-\upsilon^2\sqrt{(x_Z^2-4r_Z)(x_1^2-4r_H)}\cos\theta\cos\theta_1-(1-\upsilon^2)(y_2-z_Z)], \quad (10)$$

$$f_2=-\upsilon^2(x_Z^2-4r_Z)\sin^2\theta\cos(2\varphi-\Phi)-\left(2-\frac{y_1+r_H}{r_Z}+\frac{(y_1+r_Z)^2}{4r_Z^2}\right)[\upsilon^2(x_1^2-4r_H)\sin^2\theta_1\cos(2\varphi-\Phi)+$$
$$+\frac{y_1+r_Z}{r_Z}\left[\cos\Phi(x_Zx_1-\upsilon^2\sqrt{(x_Z^2-4r_Z)(x_1^2-4r_H)}\cos\theta\cos\theta_1-\frac{1+\upsilon^2}{2}\sqrt{(x_Z^2-4r_Z)(x_1^2-4r_H)}\times\right.$$
$$\left.\times\sin\theta\sin\theta_1(\cos\Phi+\cos(2\varphi-\Phi))-(1+\upsilon^2)(y_2-r_Z)\cos\Phi\right], \quad (11)$$

λ_1 and λ_2 (η_1 and η_2) – the helicity (transverse components of spin vectors) of the electron and positron, $d\Omega=\sin\theta d\theta d\varphi$ – the solid angle of departure of the Z-boson, $\theta(\theta_1)$ – the angle between the directions of the momentums of the electron $\vec{p}_1$ and the Z-boson $\vec{k}$ (Higgs boson $\vec{k}_1$), $\upsilon=\sqrt{1-4m^2/s}$ – the velocity of the electron in the center of mass system, $\vec{p}_1+\vec{p}_2=\vec{k}+\vec{k}_1+\vec{k}_2=0$ because of which the final particles lie in the same plane with the azimuthal angle φ.

It should be noted that the electron momentum $\vec{p}_1$ is directed along the axis Z, and its spin vector $\vec{\eta}_1$ is along the axis X, then the spin vector $\vec{\eta}_2$ will lie in the plane XOY, the angle between the transverse components of the spin vectors $\vec{\eta}_1$ and $\vec{\eta}_2$ is denoted by Φ.

We now proceed to the calculation of the diagram d), the amplitude of which can be written as follows:

$$M_d = g_{Zee} g^2_{ZZH} \frac{1}{s(1-r_Z)} \frac{1}{s(y_2 + r_H - r_Z)} \ell_\nu \left(g_{\nu\rho} - \frac{q'_\nu q'_\rho}{M_Z^2} \right) U^*_\rho(k), \tag{12}$$

where $q'_\nu = (p - k_2)_\nu = (k + k_1)_\nu$ is the total 4-momentum Z - and Higgs bosons. Based on this amplitude, the following expression is obtained for the differential effective cross section of the reaction $e^-e^+ \to ZHH$:

$$\frac{d^3\sigma_d}{dx_Z dx_1 d\Omega} = \frac{\sqrt{2}}{128\pi^4} \cdot \frac{G_F^3 M_Z^6}{s(1-r_Z)^2} \cdot \frac{r_Z}{(y_2 + r_H - r_Z)^2} \times$$
$$\times \{[(g_L^2(1-\lambda_1)(1+\lambda_2) + g_R^2(1+\lambda_1)(1-\lambda_2)] \cdot F_1 + 2 g_L g_R \eta_1 \eta_2 F_2]\}, \tag{13}$$

where the functions F_1 and F_2 are obtained from the functions f_1 and f_2 (expressions (10) and (11)) using substitutions

$$\theta_1 \to \theta_2,\ x_1 \to x_2,\ y_1 \to y_2.$$

The square of the amplitude corresponding to the interference of diagrams c) and d)

$$M_c^+ M_d + M_d^+ M_c = 2 \frac{g^2_{Zee}}{s^2(1-r_Z)^2} \frac{g^4_{ZZH}}{s^2(y_1 + r_H - r_Z)(y_2 + r_H - r_Z)} \times$$
$$\times L_{\mu\nu} \left[-g_{\mu\nu} + \frac{k_\mu k_\nu}{M_Z^2} + \frac{k_{1\mu} k_{1\nu}}{M_Z^2} + \frac{k_{2\mu} k_{2\nu}}{M_Z^2} - \frac{k_\mu k_{1\nu} + k_{1\mu} k_\nu}{2M_Z^2} \frac{y_2 - r_Z}{2r_Z} - \frac{k_\mu k_{2\nu} + k_{2\mu} k_\nu}{2M_Z^2} \frac{y_1 - r_Z}{2r_Z} - \right.$$
$$\left. - \frac{k_{1\mu} k_{2\nu} + k_{2\mu} k_{1\nu}}{2M_Z^2} \frac{1}{2r_Z} \left(y_Z + r_Z - 2r_H - \frac{y_1 - r_Z}{2r_Z} (y_2 - r_Z) \right) \right] \tag{14}$$

it has a bulky appearance, so it is not given here.

Based on the matrix element (14) for the contribution to the cross-section of the interference process $e^-e^+ \to ZHH$ of diagrams c) and d), we obtain the expression (angle Φ accepted π):

$$\frac{d^3\sigma^{(\text{inter.})}_{c,d}}{dx_Z dx_1 d\Omega} = \frac{\sqrt{2}}{64\pi^4} \cdot \frac{G_F^3 M_Z^6}{s(1-r_Z)^2} \cdot \frac{r_Z}{(y_1 + r_H - r_Z)(y_2 + r_H - r_Z)} \left\{ g_L^2(1-\lambda_1)(1+\lambda_2) + g_R^2(1+\lambda_1)(1-\lambda_2)] \times \right.$$
$$\times \left[x_Z^2 \sin^2\theta + 4r_Z(1 + \cos^2\theta) + (x_1^2 - 4r_H)\sin^2\theta_1 + (x_2^2 - 4r_H)\sin^2\theta_2 - \right.$$
$$- \frac{y_2 - r_Z}{2r_Z} (x_Z x_1 - \sqrt{(x_Z^2 - 4r_Z)(x_1^2 - 4r_H)} \cdot \cos\theta \cos\theta_1 - 2(y_2 - r_Z)) -$$
$$- \frac{y_1 - r_Z}{2r_Z} (x_Z x_2 - \sqrt{(x_Z^2 - 4r_Z)(x_2^2 - 4r_H)} \cdot \cos\theta \cos\theta_2 - 2(y_1 - r_Z)) -$$
$$- \frac{1}{2r_Z} (x_1 x_2 - \sqrt{(x_1^2 - 4r_H)(x_2^2 - 4r_H)} \cdot \cos\theta_1 \cos\theta_2 - 2(y_Z + r_Z - 2r_H) \times$$
$$\left. \times \left(y_Z + r_Z - 2r_H - \frac{1}{2r_Z} (y_1 - r_Z)(y_2 - r_Z) \right) \right] + 2 g_L g_R \eta_1 \eta_2 \left[((x_Z^2 - 4r_Z)\sin^2\theta + \right.$$
$$+ (x_1^2 - 4r_H)\sin^2\theta_1 - (x_2^2 - 4r_H)\sin^2\theta_2)\cos 2\varphi + \frac{y_2 - r_Z}{2r_Z} (x_Z x_1 - \sqrt{(x_Z^2 - 4r_Z)(x_1^2 - 4r_H)} \times$$
$$\times \cos(\theta - \theta_1) - 2(y_2 - r_Z)) - \sqrt{(x_Z^2 - 4r_Z)(x_1^2 - 4r_H)} \cdot \sin\theta \sin\theta_1 \cos(2\varphi) +$$
$$+ \frac{y_1 - r_Z}{2r_Z} (x_Z x_2 - \sqrt{(x_Z^2 - 4r_Z)(x_2^2 - 4r_H)} \cdot \cos(\theta - \theta_2) - 2(y_1 - r_Z) - \sqrt{(x_Z^2 - 4r_Z)(x_2^2 - 4r_H)} \times$$
$$\left. \left. \times \cos(\theta_1 - \theta_2) - 2(y_Z + r_Z - 2r_H) - \sqrt{(x_1^2 - 4r_H)(x_2^2 - 4r_H)} \cdot \sin\theta_1 \sin\theta_2 \cos(2\varphi) \right) \right] \right\}. \tag{15}$$

3. CALCULATION OF INTERFERENCE DIAGRAMS a), b) AND c), d)

During annihilation of an arbitrarily polarized electron-positron pair for interference diagram a), b) and c),

d), the following expressions are obtained:

$$\frac{d^3\sigma_{a,c}^{(\text{inter.})}}{dx_Z dx_1 d\Omega}=\frac{3\sqrt{2}}{128\pi^4}\cdot\frac{G_F^3 M_Z^6}{s(1-r_Z)^2}\cdot\frac{r_H}{y_Z+r_Z-r_H}\cdot\frac{1}{y_1+r_H-r_Z}\times$$
$$\times\{-[g_L^2(1-\lambda_1)(1+\lambda_2)+g_R^2(1+\lambda_1)(1-\lambda_2)][x_Z^2\sin^2\theta+4r_Z(1+\cos^2\theta)+(x_1^2-4r_H)\sin^2\theta_1+$$
$$+\frac{y_1+r_Z}{2r_Z}\cdot(x_Z x_1-\sqrt{(x_Z^2-4r_Z)(x_1^2-4r_H)}\cos\theta\cos\theta_1-2(y_2-r_Z))]+$$
$$+2g_L g_R\eta_1\eta_2[-(x_Z^2-4r_Z)\sin^2\theta\cos(2\varphi)-(x_1^2-4r_H)\sin^2\theta_1\cos(2\varphi)+$$
$$+\frac{y_1+r_Z}{2r_Z}(x_Z x_1-\sqrt{(x_Z^2-4r_Z)(x_1^2-4r_H)}\cos(\theta-\theta_1)-2(y_2-r_Z)-$$
$$-\sqrt{(x_Z^2-4r_Z)(x_1^2-4r_H)}\sin\theta\sin\theta_1\cos(2\varphi))]\}; \qquad (16)$$

$$\frac{d^3\sigma_{a,d}^{(\text{inter})}}{dx_Z dx_1 d\Omega}=\frac{3\sqrt{2}}{128\pi^4}\cdot\frac{G_F^3 M_Z^6}{s(1-r_Z)^2}\cdot\frac{r_H}{y_Z+r_Z-r_H}\cdot\frac{1}{y_2+r_H-r_Z}\times$$
$$\times\{-[g_L^2(1-\lambda_1)(1+\lambda_2)+g_R^2(1+\lambda_1)(1-\lambda_2)][x_Z^2\sin^2\theta+4r_Z(1+\cos^2\theta)+$$
$$+(x_2^2-4r_H)\sin^2\theta_2+\frac{y_2+r_Z}{2r_Z}\cdot(x_Z x_2-\sqrt{(x_Z^2-4r_Z)(x_2^2-4r_H)}\cos\theta\cos\theta_2-2(y_1-r_Z))]+$$
$$+2g_L g_R\eta_1\eta_2[-((x_Z^2-4r_Z)\sin^2\theta\cos(2\varphi)-(x_2^2-4r_H)\sin^2\theta_2)\cos(2\varphi)+$$
$$+\frac{y_2+r_Z}{2r_Z}(x_Z x_2-\sqrt{(x_Z^2-4r_Z)(x_2^2-4r_H)}\cos(\theta-\theta_2)-2(y_1-r_Z))-$$
$$-\sqrt{(x_Z^2-4r_Z)(x_2^2-4r_H)}\sin\theta\sin\theta_2\cos(2\varphi))]\}; \qquad (17)$$

$$\frac{d^3\sigma_{b,c}^{(\text{inter})}}{dx_Z dx_1 d\Omega}=\frac{\sqrt{2}G_F^3 M_Z^6}{256\pi^4}\cdot\frac{1}{s(1-r_Z)^2}\cdot\frac{1}{y_1+r_H-r_Z}\cdot\frac{r_H}{r_Z}\times$$
$$\times\{-[g_L^2(1-\lambda_1)(1+\lambda_2)+g_R^2(1+\lambda_1)(1-\lambda_2)][x_Z^2\sin^2\theta+4r_Z(1+\cos^2\theta)+$$
$$+(x_1^2-4r_H)\sin^2\theta_1+\frac{y_2+r_Z}{2r_Z}(x_Z x_1-\sqrt{(x_Z^2-4r_Z)(x_1^2-4r_H)}\cos\theta\cos\theta_1-2(y_2-r_Z))]+$$
$$+2g_L g_R\eta_1\eta_2[-((x_Z^2-4r_Z)\sin^2\theta\cos(2\varphi)-(x_1^2-4r_H)\sin^2\theta_1)\cos(2\varphi)+$$
$$+\frac{y_1+r_Z}{2r_Z}(x_Z x_1-\sqrt{(x_Z^2-4r_Z)(x_1^2-4r_H)}\cos(\theta-\theta_1)-2(y_2-r_Z))-$$
$$-\sqrt{(x_Z^2-4r_Z)(x_1^2-4r_H)}\sin\theta\sin\theta_1\cos(2\varphi))]\}; \qquad (18)$$

$$\frac{d^3\sigma_{b,d}^{(\text{inter})}}{dx_Z dx_1 d\Omega}=\frac{\sqrt{2}G_F^3 M_Z^6}{256\pi^4}\cdot\frac{1}{s(1-r_Z)^2}\cdot\frac{1}{y_2+r_H-r_Z}\cdot\frac{r_H}{r_Z}\times$$
$$\times\{-[g_L^2(1-\lambda_1)(1+\lambda_2)+g_R^2(1+\lambda_2)(1-\lambda_1)][x_Z^2\sin^2\theta+4r_Z(1+\cos^2\theta)+$$
$$+(x_2^2-4r_H)\sin^2\theta_2+\frac{y_2+r_Z}{2r_Z}\cdot(x_Z x_2-\sqrt{(x_Z^2-4r_Z)(x_2^2-4r_H)}\cos\theta\cos\theta_2-$$
$$-2(y_1-r_Z))]+2g_L g_R\eta_1\eta_2[(-(x_Z^2-4r_Z)\sin^2\theta-(x_2^2-4r_H)\sin^2\theta_2)\cos(2\varphi)+$$
$$+\frac{y_2+r_Z}{2r_Z}(x_Z x_2-\sqrt{(x_Z^2-4r_Z)(x_2^2-4r_H)}\cos(\theta-\theta_2)-2(y_1-r_H))-$$
$$-\sqrt{(x_Z^2-4r_Z)(x_2^2-4r_H)}\sin\theta\sin\theta_2\cos(2\varphi))]\} \qquad (19)$$

Thus, we calculated the differential effective cross section of the reaction $e^-e^+ \to ZHH$ taking into account all Feynman diagrams (Fig. 1, a, b, c, d). This section contains the contributions of diagrams a), b) and their interferences (they are given in (I) work), the contributions of diagrams c), d) and their interferences (formulas (9), (13) and (15)), as well as the interferences of diagrams a) and c), a) and d), b) and c), b) and d) (formulas (16)-(19)).

4. LEFT-RIGHT AND TRANSVERSE SPIN ASYMMETRIES

Consider left-right A_{LR} and transverse $A_\varphi(x_Z,\theta)$ spin asymmetries taking into account all Feynman diagrams. In all expressions of the differential effective cross sections given above, the helicity of the electron and positron are in the form

$$[g_L^2(1-\lambda_1)(1+\lambda_2)+g_R^2(1+\lambda_1)(1-\lambda_2)],$$

consequently, the left-right spin asymmetry due to the longitudinal polarization of the electron is expressed by the formula

$$A_{LR}=\frac{g_L^2-g_R^2}{g_L^2+g_R^2}. \tag{20}$$

As can be seen, the left-right spin asymmetry A_{LR} depends only on the Weinberg parameter x_W and with the value of this parameter $x_W=0.2315$ is $A_{LR}=14\%$.

As for the transverse spin asymmetry $A_\varphi(x_Z,\theta)$, we estimate it at the value of the Higgs boson energy $x_1=0.5$ according to the formula

$$A_\varphi(x_Z,\theta)=\frac{2g_Lg_R}{g_L^2+g_R^2}\cdot\frac{\psi_2}{\psi_1}, \tag{21}$$

where the functions ψ_1 and ψ_2 are equal:

$$\psi_1=\frac{1}{4r_Z}\left(1-\frac{3r_H}{y_Z+r_Z-r_H}\right)^2[x_Z^2\sin^2\theta+4r_Z(1+\cos^2\theta)]+$$

$$+\frac{r_Z}{(y_1+r_H-r_Z)^2}\cdot[x_Z^2\sin^2\theta+4r_Z(1+\cos^2\theta)+\frac{y_1+r_Z}{r_Z}(x_Zx_1-2(y_2-r_Z))]+$$

$$+\frac{r_Z}{(y_2+r_H-r_Z)^2}\cdot\left[x_Z^2\sin^2\theta+4r_Z(1+\cos^2\theta)+\left(2-\frac{y_1+r_H}{r_Z}+\frac{(y_1+r_Z)^2}{4r_Z^2}\right)\times\right.$$

$$\times(x_2^2-4r_H)\sin^2\theta_2+\frac{y_2+r_Z}{r_Z}\cdot(x_Zx_2-\sqrt{(x_Z^2-4r_Z)(x_2^2-4r_H)}\cos\theta\cos\theta_2-$$

$$\left.-2(y_1-r_Z))\right]+\frac{2}{y_1+r_H-r_Z}\cdot\frac{r_Z}{(y_2+r_H-r_Z)}\cdot\left[x_Z^2\sin^2\theta+4r_Z(1+\cos^2\theta)+\right.$$

$$+(x_2^2-4r_H)\sin^2\theta_2-\frac{y_2-r_Z}{2r_Z}(x_Zx_1-2(y_2-r_Z))-\frac{y_1-r_Z}{2r_Z}\cdot(x_Zx_2-$$

$$-\sqrt{(x_Z^2-4r_Z)(x_2^2-4r_H)}\cos\theta\cos\theta_2-2(y_1-r_Z))-\frac{1}{2r_Z}(x_1x_2-2(y_Z+r_Z-2r_H))\times$$

$$\left.\times\left(y_Z+r_Z-2r_H-\frac{1}{2r_Z}(y_1-r_Z)(y_2-r_Z)\right)\right]-\frac{3}{y_Z+r_Z-r_H}\cdot\frac{r_H}{y_1+r_H-r_Z}\times$$

$$\times\left[x_Z^2\sin^2\theta+4r_Z(1+\cos^2\theta)+\frac{y_1+r_Z}{2r_Z}(x_Zx_1-2(y_2-r_Z))\right]-$$

$$-\frac{3}{y_Z+r_Z-r_H}\cdot\frac{r_H}{y_2+r_H-r_Z}\left[x_Z^2\sin^2\theta+4r_Z(1+\cos^2\theta)+(x_2^2-4r_H)\sin^2\theta_2+\right.$$

$$\left.+\frac{y_2+r_Z}{2r_Z}(x_Zx_2-\sqrt{(x_Z^2-4r_Z)(x_2^2-4r_H)}\cos\theta\cos\theta_2-2(y_1-r_Z))\right]-$$

$$-\frac{r_H}{2r_Z}\cdot\frac{1}{y_1+r_H-r_Z}\left[x_Z^2\sin^2\theta+4r_Z(1+\cos^2\theta)+\frac{y_1+r_Z}{2r_Z}(x_Zx_1-2(y_2-r_H))\right]-$$

$$-\frac{r_H}{2r_Z}\cdot\frac{1}{y_2+r_H-r_Z}\Bigg[x_Z^2\sin^2\theta+4r_Z(1+\cos^2\theta)+(x_2^2-4r_H)\sin^2\theta_2+$$

$$+\frac{y_2+r_Z}{2r_Z}\cdot(x_Zx_2-\sqrt{(x_Z^2-4r_Z)(x_2^2-4r_H)}\cos\theta\cos\theta_2-2(y_1-r_Z))\Bigg]; \qquad (22)$$

$$\psi_2=\frac{1}{4r_Z}\left(1-\frac{3r_H}{y_Z+r_Z-r_H}\right)^2[(x_Z^2-4r_Z)\sin^2\theta\cos2\varphi+$$

$$+\frac{r_Z}{(y_1+r_H-r_Z)^2}\cdot[(x_Z^2-4r_Z)\sin^2\theta\cos2\varphi+\frac{y_1+r_Z}{r_Z}(-x_Zx_1+2(y_2-r_Z))]+$$

$$+\frac{r_Z}{(y_2+r_H-r_Z)^2}\cdot\Bigg[(x_Z^2-4r_Z)\sin^2\theta\cos2\varphi+\left(2-\frac{y_1+r_H}{r_Z}+\frac{(y_1+r_Z)^2}{4r_Z^2}\right)\times$$

$$\times(x_2^2-4r_H)\sin^2\theta_2\cos2\varphi+\frac{y_2+r_Z}{r_Z}\cdot(-x_Zx_2+\sqrt{(x_Z^2-4r_Z)(x_2^2-4r_H)}\times$$

$$\times(\cos\theta\cos\theta_2+\sin\theta\sin\theta_2(1+\cos2\varphi)+2(y_1-r_Z))\Bigg]+$$

$$+\frac{2}{y_1+r_H-r_Z}\cdot\frac{r_Z}{y_2+r_H-r_Z}\cdot\Bigg[\cos2\varphi((x_Z^2-4r_Z)\sin^2\theta-(x_2^2-4r_H)\sin^2\theta_2)+$$

$$+\frac{y_2-r_Z}{2r_Z}\cdot(x_Zx_1-2(y_2-r_Z))+\frac{y_1-r_Z}{2r_Z}\cdot(x_Zx_2-\sqrt{(x_Z^2-4r_Z)(x_2^2-4r_H)}\cos(\theta-\theta_2)-$$

$$-2(y_1-r_Z)-\sqrt{(x_Z^2-4r_Z)(x_2^2-4r_H)}\cdot\sin\theta\sin\theta_2\cos2\varphi)+$$

$$+\frac{1}{2r_Z}\left(y_Z+r_Z-2r_H-\frac{(y_1-r_Z)(y_2-r_Z)}{2r_Z}\right)\cdot(x_1x_2-2(y_Z+r_Z-2r_H))\Bigg]+\frac{3}{y_Z+r_Z-r_H}\cdot$$

$$\times\frac{r_H}{y_1+r_H-r_Z}\cdot\Bigg[-(x_Z^2-4r_Z)\sin^2\theta\cos\theta2\varphi+\frac{y_1+r_Z}{2r_Z}(x_Zx_1-2(y_2-r_Z))\Bigg]+$$

$$+\frac{3}{y_Z+r_Z-r_H}\cdot\frac{r_H}{y_2+r_Z-r_H}\cdot\Bigg[\cos2\varphi(-(x_Z^2-4r_Z)\sin^2\theta-(x_2^2-4r_H)\sin^2\theta_2)+$$

$$+\frac{y_2+r_Z}{2r_Z}(x_Zx_2-\sqrt{(x_Z^2-4r_Z)(x_2^2-4r_H)}\cos(\theta-\theta_2)-2(y_1-r_Z)-$$

$$-\sqrt{(x_Z^2-4r_Z)(x_2^2-4r_H)}\cdot\sin\theta\sin\theta_2\cos2\varphi)\Bigg]+$$

$$+\frac{r_H}{2r_Z}\cdot\frac{1}{y_1+r_H-r_Z}\Bigg[-(x_Z^2-4r_Z)\sin^2\theta\cos2\varphi+\frac{y_1+r_Z}{2r_Z}(x_Zx_1-2(y_2-r_Z))\Bigg]+$$

$$+\frac{r_H}{2r_Z}\cdot\frac{1}{y_2+r_H-r_Z}[\cos2\varphi(-(x_Z^2-4r_Z)\sin^2\theta-(x_2^2-4r_H)\sin^2\theta_2]+$$

$$+\frac{y_2+r_Z}{2r_Z}(x_Zx_2-\sqrt{(x_Z^2-4r_Z)(x_2^2-4r_H)}\cos(\theta-\theta_2)-2(y_1-r_H)-$$

$$-\sqrt{(x_Z^2-4r_Z)(x_2^2-4r_H)}\cdot\sin\theta\sin\theta_2\cos2\varphi)]. \qquad (23)$$

When obtaining these formulas, we took into account that at $x_1=0.5$ $x_1^2-4r_H=0$ and the angle θ_2 between the momentums of the electron and the second Higgs boson $\vec{k}_2$ is related to the angle θ by the ratio

$$\cos\theta_2=-\sqrt{\frac{x_Z^2-4r_Z}{x_2^2-4r_H}}\cos\theta.$$

Figure 2 shows the dependence of the transverse spin asymmetry $A_\varphi(x_Z,\theta)$ on the angle θ at different energy values x_Z: 1) $x_Z=0.55$; 2) $x_Z=0.60$; 3) $x_Z=0.65$. As can be seen from the figure, the transverse spin asymmetry is positive and at $x_Z=0.55$ and $x_Z=0.60$ with increasing angle θ, it decreases and reaches a minimum at an angle of $\theta=90°$, and with further increase in angle, the transverse spin asymmetry increases. At x_Z=0.65, an increase in the angle θ leads to an increase in the transverse spin asymmetry, it reaches a maximum at $\theta=90°$, and then decreases.

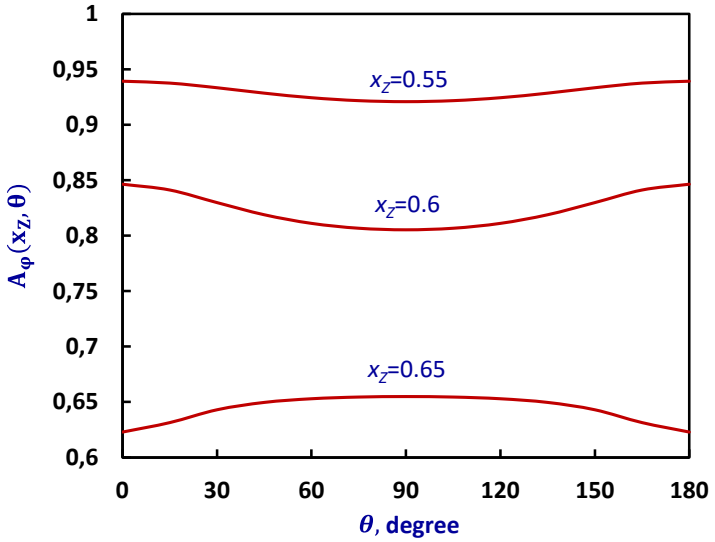

Fig. 2. Angular dependence of transverse spin asymmetry at different x_Z

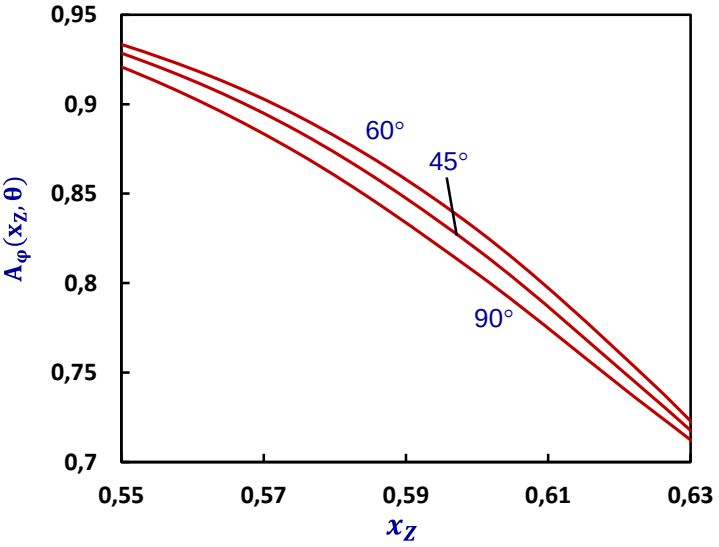

Fig. 3. Energy dependence of transverse spin asymmetry at different angles θ

Fig. 3 illustrates the dependence of the transverse spin asymmetry on the fraction of energy x_Z carried away by the Z^0-boson at different departure angles θ: 1) $\theta = 45°$; 2) $\theta = 60°$; 3) $\theta = 90°$. It follows from the figure that with increasing x_Z the transverse spin asymmetry monotonically decreases.

Averaging over the polarization states e^-e^+-pairs for the differential effective cross section of the reaction $e^-e^+ \to HHZ^0$ we have the formula (all Feynman diagrams are taken into account)

$$\frac{d^3\sigma}{dx_Z dx_1 d\Omega} = \frac{\sqrt{2}}{128\pi^4} \frac{G_F^3 M_Z^6}{s} \cdot \frac{1}{(1-r_Z)^2} \cdot \psi_1, \qquad (24)$$

where the function ψ_1 is given by formula (22).

Figure 4 shows the angular dependence of the differential effective cross section of the reaction $e^-e^+ \to HHZ^0$ at $\sqrt{s} = 500$ GeV, $x_1 = 0.5$, $x_W = 0.2315$ and various energy values x_Z: 1) $x_Z = 0.65$; 2) $x_Z = 0.70$; 3) $x_Z = 0.75$. As can be seen from the figure, with an increase in the polar angle θ, the differential effective cross-section increases and reaches a maximum at an angle of $\theta = 90°$, and with a further increase in the same angle, the effective cross-section decreases. An increase in the energy x_Z carried away by the Z^0-boson leads to an increase in the effective cross-section of the process under study.

Fig. 5 illustrates the dependence of the cross section of the process $e^-e^+ \to HHZ^0$ on the variable x_Z at $\sqrt{s} = 500$ GeV, $x_1 = 0.5$ and various values of the departure angle θ: 1) $\theta = 30°$; 2) $\theta = 60°$; 3) $\theta = 90°$. It can be seen from the figure that with an increase in the energy x_Z carried away by the Z^0-boson, the effective cross-section increases, the increase in the departure angle θ also leads to an increase in the effective cross-section of the process under consideration.

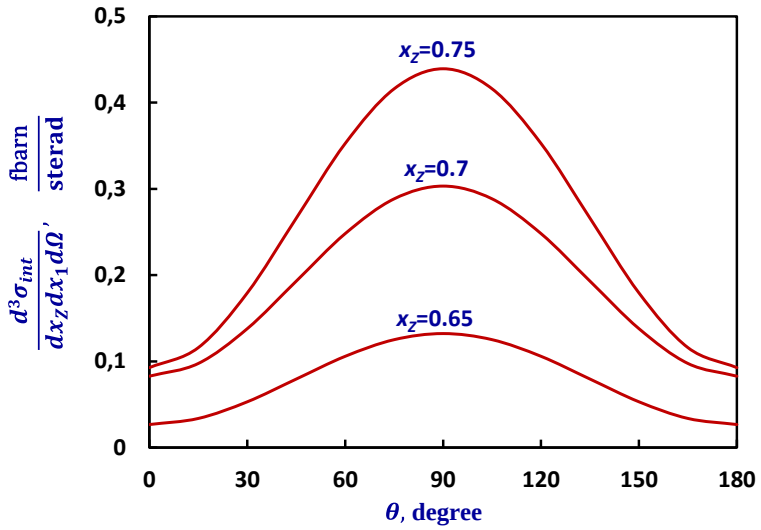

Fig. 4. Angular dependence of the cross section the process $e^-e^+ \to HHZ^0$ at different energy values x_Z

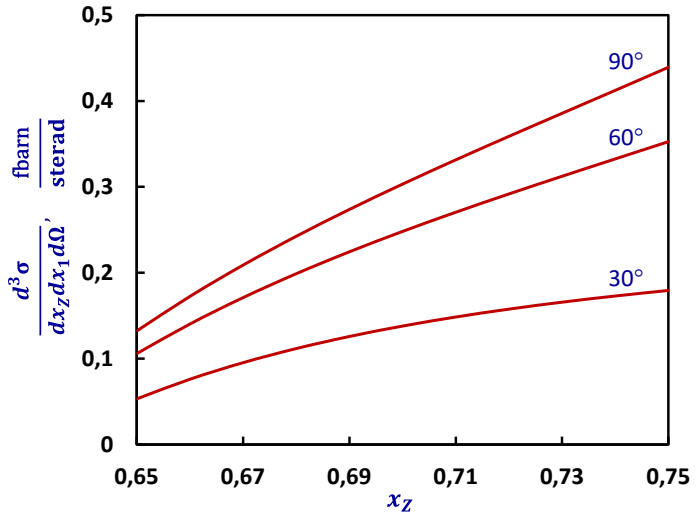

Fig. 5. Energy dependence of the cross section of process $e^-e^+ \to HHZ^0$ at different angles of θ

By averaging over the polarization states of the electron-positron pair and integrating over the departure angles of the particles, for the energy distribution of the Higgs bosons we obtain the formula

$$\frac{d^2\sigma}{dx_1 dx_2} = \frac{G_F^3 M_Z^6}{48\sqrt{2}\pi^3} \cdot \frac{g_L^2 + g_R^2}{s(1-r_Z)^2} \cdot \psi, \tag{25}$$

where

$$\psi = \frac{\varphi_0}{8} b^2 + \frac{1}{4r_Z(y_1 + r_H - r_Z)} \left[\frac{\varphi_1}{y_1 + r_H - r_Z} + \frac{\varphi_2}{y_2 + r_H - r_Z} + 2r_Z b \varphi_3 \right] + \{y_1 \leftrightarrow y_2\}, \tag{26}$$

$$b = \frac{\lambda_{HHH}}{y_3 - r_H + r_Z} + \frac{2}{y_1 + r_H - r_Z} + \frac{2}{y_2 + r_H - r_Z} + \frac{1}{r_Z}, \tag{27}$$

$$\varphi_0 = r_Z[(y_1 + y_2)^2 + 8r_Z],$$

$$\varphi_1 = (y_1 - 1)^2 (r_Z - y_1)^2 - 4r_H y_1 (y_1 + y_1 r_Z - 4r_Z) + r_Z (r_Z - 4r_H)(1 - 4r_H) - r_Z^2,$$

$$\varphi_2 = [r_Z(y_3 + r_Z - 8r_H) - (1 + r_Z) y_1 y_2](1 + y_3 + 2r_Z) + y_1 y_2 [y_1 y_2 + 1 + r_Z^2 + 4r_H(1 + r_Z)] +$$

$$+ 4r_H r_Z (1 + r_Z + 4r_H) + r_Z^2,$$

$$\varphi_3 = y_1(y_1 - 1)(r_Z - y_1) - y_2(y_1 + 1)(y_1 + r_Z) + 2r_Z(1 + r_Z - 4r_H).$$

Figure 6 shows the dependence of the differential effective cross section (25) on the scaling energy x_1 at $\sqrt{s} = 500$ GeV and various values of the variable x_2: 1) x_2 =0.65; 2) x_2 =0.75; 3) x_2 =0.85. As can be seen from the figure, at x_2 =0.85, the differential effective cross-section increases with the growth of the variable x_1, and at x_2 =0.75 (x_2 =0.65), the effective cross-section first decreases and reaches a minimum at x_1=0.67 (x_1=0.73), and then with an increase of x_1 it begins to grow. In the case of x_2 =0.85 and x_1=0.8, the cross-section of the process is 2.23 fbarn.

5. CONCLUSION

In conclusion, we note that the experimental study of the reaction of the association production of a Higgs boson pair and a vector Z^0-boson in electron-positron annihilation is of great interest, since it allows measuring the interaction constants of three Higgs bosons g_{HHH} and two Z^0 - and two Higgs bosons g_{ZZHH}.

Although the interaction constants of vector bosons with the Higgs boson g_{ZZH} and g_{WWH} are measured in the LHC in proton-proton collisions, however, direct measurement of the interaction constants g_{HHH} and g_{ZZHH} is associated with certain difficulties. Therefore, the study of the process $e^-e^+ \to HHZ^0$ is of particular interest.

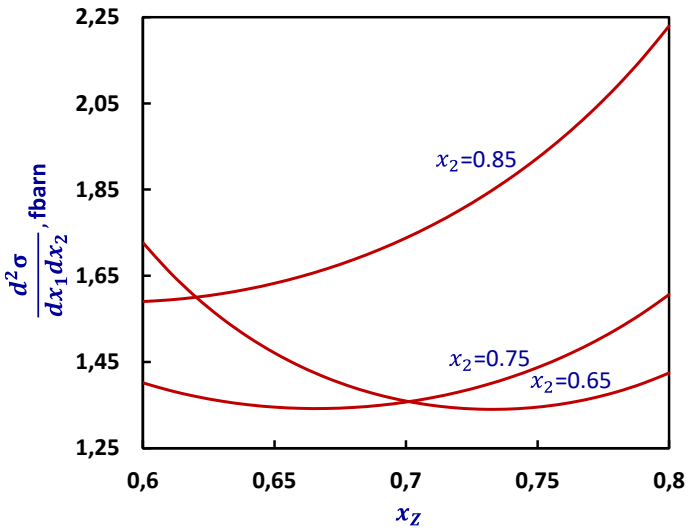

Fig. 6. Energy dependence of the reaction $e^-e^+ \to HHZ^0$ cross section at different values x_2.

We discussed the process of the production of a vector Z^0-boson and two Higgs boson pairs in polarized electron-positron collisions $e^-e^+ \to HHZ^0$. Taking into account all possible Feynman diagrams a), b), c) and d) Fig. 1, analytical expressions for the amplitudes and differential effective cross section of the process are obtained. Left-right A_{LR} and transverse spin asymmetries A_φ due to longitudinal and transverse polarizations of the electron-positron pair are determined. The dependence of these characteristics and the differential effective cross-section on the departure angles and particle energies is studied in detail. The calculation results are illustrated with graphs.

[1] *A.A. Sokolov, I.M. Ternov, V.Ch. Zhukovsky, A.V. Borisov*. Calibration fields. Moscow: Publishing House of MSU, 1986. 260 p. (in Russian).

[2] *A. Djouadi*. The Anatomy of Electro-Weak Symmetry Breaking. Tome I: The Higgs boson in the Standard Model. arXiv: hep-ph/0503172v2, 2005.

[3] *S.K. Abdullayev*. Standard Model, properties of leptons and quarks. Baku, 2017. 276 p. (in Azerb.)

[4] ATLAS Collaboration. Observation of a new particle in the search for the Standard Model Higgs boson with the ATLAS detector of the LHC. Phys. Letters, 2012, B 716, p. 1-29.

[5] CMS Collaboration. Observation of a new boson at mass of 125 GeV with the CMS experiment at the LHC. Phys. Letters, 2012, B 716, p. 30-60.

[6] *V.A. Rubakov*. On Large Hadron Colliders discovery of a new particle with Higgs Boson properties. UFN, 2012, V.182, No 10, p.1017-1025 (in Russian).

[7] *D.I. Kazakov*. The Higgs boson is found: what is next? UFN, 2014, V. 184, No 9, p. 1004-1017 (In Russian).

[8] *A.V. Lanev*. CMS Collaboration results: Higgs boson and search for new physics. UFN, 2014, V. 184, No 9, p. 996-1004 (In Russian).

[9] *V.D. Shiltsev*. High energy particle colliders:

past 20 years, next 20 years and beyond. UFN, 2012, V. 182, No 10, p. 1033-1046. (in Russian).

[10] *K. Peters*. Prospects for beyond Standard Model Higgs boson searches at future LHC runs and other machines. arXive: 1701.05124v2 [hep-ex], 2007, 8p.

[11] *W. Kilian, M. Kramer, P. Zerwas*. Higgs-strahlung and WW fusion in e^+e^--collisions. Phys. Lett. B373, 1996, p. 135-140.

[12] *M. Greco, G. Montagna, O. Nicrosini, F. Piccinini, G. Volpi*. ISR corrections to associated HZ production at future Higgs factories. Phys. Lett. 2018. v. B777. P. 294-297.

[13] *M. Greco, T. Han, Z. Lio*. ISR effects for resonant Higgs production at future lepton colliders. Phys. Lett. 2016, v. B763, p. 409-415.

[14] *Y. Gong, Z. Li, X. Xu, L. Yang, X. Zhao*. Mixed QCD-electroweak corrections for Higgs boson production at e^+e^--colliders. Phys. Rev., 2017, v. D 95 (9), p. 093003.

[15] *A. Djouadi, W. Kilian, M. Mühlleitner, P.M. Zerwas*. Testing Higgs self-couplings at e^+e^--linear colliders. Eur. Phys. J. C Particles and Fields, 1999, v. 10, p. 27-43.

[16] *V. Barger, T. Han, P. Langacker, B. McElrath, P. Zerwas*. Effects of genuine dimension-six Higgs operators. Phys. Rev., 2003, v. D67, p. 115001.

[17] S.*K. Abdullayev, M.Sh. Gojayev*. Production of a Higgs-boson pair in e^+e^--collisions (I). Izv. VUZov. Fizika, 2022, т. 65, № 8, с. 28-36 (In Russian).

Received: 29.12.2022